International Journal for Housing Science and Its Applications
Publish August 10, 2025. Volume 46, Issue 4 Pages 15-28

https://doi.org/10.70517/ijhsa46402

Research on resource aggregation scheduling and optimization control strategy of virtual power plant based on spatio-temporal data mining computational analysis

Zongchen Li[1,*]
[1] Modern Education Center of ChangChun Finance College, Changchun, Jilin, 130124, China
Corresponding authors: (e-mail: lizongchen6903@163.com).

Abstract In recent years, virtual power plants have rapidly emerged as a flexible and efficient form of intelligent energy management. This paper focuses on the optimal scheduling of virtual power plant resources, after explaining the virtual power plant resources and their characteristics, it proposes a new energy consumption model of virtual power plant with hybrid energy storage system, establishes a joint optimal scheduling model of thermoelectricity and electricity based on the hybrid storage system, and selects the improved particle swarm algorithm for the optimization and solving. Collecting the relevant spatio-temporal data of the system power generation for example analysis, the improved particle swarm algorithm has better convergence, and the optimal allocation of energy storage is realized when the electric energy storage and thermal energy storage are 9MWh and 35MWh, respectively, and then the annual profit of the virtual power plant can be increased by 605,610,000 yuan. In addition, after the aggregated scheduling of the model, the electric load demand response and the electric energy storage work together to maintain the balance of the electric output of the virtual power plant. The proposed optimization control strategy can realize the complementary advantages of distributed resources, improve the flexible regulation ability of the virtual power plant, alleviate the pressure of power supply preservation, and ensure the safe and smooth operation of the power grid.

Index Terms particle swarm algorithm, resource optimal scheduling, combined heat and power, virtual power plant

I. Introduction

In the context of dual-carbon targets and the construction of new power systems, the increasing penetration of renewable energy sources and the decreasing regulation capacity of resources on the traditional generation side have led to a significant increase in the flexibility needs of the power system [1]-[3]. At the same time, the problem of wind and light abandonment due to the excess of renewable energy can bring serious economic losses [4], [5]. The participation of flexible load-side regulation resources in scheduling can significantly improve the flexible regulation capability of the power grid and promote the consumption of renewable energy [6], [7]. More studies have focused on introducing coupled models containing energy storage devices, electricity-to-gas, gas turbines, and other devices to increase the flexibility of system regulation, thus promoting reliable consumption of wind and light [8], [9]. However, these resources are small in capacity and large in number, and the operability of participating in grid regulation in individual form is low [10], [11]. With the popularity of distributed power applications and the increasing complexity of the system scale, realizing the coordination and optimization of distributed energy resources and improving the efficiency of energy utilization is one of the problems that need to be solved nowadays [12]-[14]. In order to fully exploit the regulation potential of flexibility resources, flexibility resources can be aggregated at scale through virtual power plants, and then flexibility resources can be efficiently and uniformly deployed on this basis [15]-[17].

The virtual power plant (VPP) can realize the organic integration of various distributed energy resources through advanced information and communication technology, so as to effectively deal with the complexity and decarbonization scheduling problems brought by the large-scale grid integration of new energy resources [18], [19]. Optimization control of virtual power plant resource scheduling refers to the use of advanced control strategies and algorithms to achieve efficient use of energy and optimization of system operation through the collaborative management and scheduling of various types of energy units within the virtual power plant [20]. The optimization and control of virtual power plants includes several aspects, such as energy production scheduling, energy storage management, and energy consumption optimization [21]-[23]. Through the use of advanced optimization algorithms and control strategies, combined with real-time monitoring data and user demand prediction, it achieves fine

regulation and optimization of each link within the virtual power plant, thus improving energy utilization efficiency, reducing energy waste, and providing technical support for the sustainable development of the smart grid [24]-[27].

The study analyzes the structure of the virtual power plant and its three resource characteristics, relying on the electric-thermal hybrid energy storage virtual power plant, taking the safe and stable operation of the virtual power plant resource system and the power grid as the premise, and taking the optimal economy and the highest utilization rate of wind and light as the optimization objectives, solves the results under the modes of equipping the heat storage tank alone, equipping the heat storage electric boiler alone, and equipping the heat storage electric boiler+heat storage tank at the same time separately, and compensates for the deviation of the output of the resources of the virtual power plant efficiently. The output deviation of virtual power plant resources is effectively compensated, and the aggregated scheduling and optimal control strategy of virtual power plant resources is proposed. The improved IEEE 30 bus system is used as an example for case study to compare the optimization effect of the improved particle swarm algorithm and genetic algorithm, and the results of energy storage allocation and optimal scheduling results of the virtual power plant are analyzed, including the specifics of electric power and thermal power, so as to test the effectiveness of the proposed optimal scheduling model for the control of the resources of the virtual power plant and the effective integration of the energy sources into the grid.

II. Characterization of virtual power plant resources

With the energy revolution, all countries are developing renewable energy, but at present, China's large-scale grid-connected renewable energy still exists in the phenomenon of water, wind and light abandonment. As an emerging technology, virtual power plant can effectively solve the problem of renewable energy consumption. This chapter introduces the basic concepts of virtual power plants and virtual power plant resources (VPP), and analyzes the characteristics of flexible loads, distributed generation resources and source loads, respectively.

II. A. Virtual power plant resources

In this paper, the virtual power plant is defined as an aggregation of fossil energy sources, renewable energy sources, distributed energy storage, flexible loads represented by demand response, and electric vehicles, which achieves energy interaction with the grid through information communication with the VPP control center, and the architecture of the virtual power plant is shown in Fig. 1. In this paper, the virtual power plant resources are categorized into three main types, which are flexible loads, distributed generation resources and source loads. Among them, flexible loads are mainly loads that can participate in demand response, distributed generation resources include renewable energy and gas turbines, and source loads include general distributed energy storage and electric vehicles.

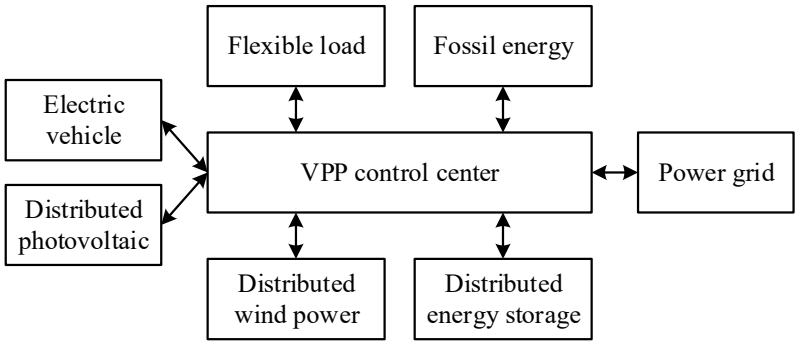

Figure 1: Architecture of virtual power plants

II. B. Power Plant Resource Characterization

II. B. 1) Flexible loads

Residential electric load is a typical flexible load. Residential load has obvious seasonality, due to the different temperatures of the four seasons, the largest load occurs in the summer, followed by winter, and the fastest annual growth of residential load is also in the summer season, followed by winter. This is due to the fact that summer and winter are more extreme, resulting in higher loads in summer and winter than in spring and fall. Typical daily loads are influenced by residents' lifestyles and work and rest schedules, with large peaks and valleys, and significant morning and evening peaks.

II. B. 2) Distributed Generation Resources

(1) Photovoltaic power generation

Photovoltaic power generation is mainly used in grid-connected operation, characterized by stochasticity and volatility, and it is generally believed that the output power changes with the intensity of solar radiation, which conforms to the Beta distribution, and its probability density function is expressed as equation (1):

$$f(r) = \frac{\Gamma(a+b)}{\Gamma(a)\Gamma(b)}\left(\frac{r}{r_{\max}}\right)^{a-1}\left(1-\frac{r}{r_{\max}}\right)^{b-1} \tag{1}$$

where $f(r)$ is the probability density function, a and b are the shape parameters of the Beta distribution, r and $r_{\max}$ denote the actual and maximum values of solar radiation intensity during the study period, respectively, and $\Gamma(\times)$ denotes the gamma function.

The PV power output varies with the solar radiation intensity, which is expressed as equation (2):

$$P_{PV}(r) = \begin{cases} P_{PVr}(r / r_{raned}) & r \le r_{raned} \\ P_{PVr} & r > r_{raned} \end{cases} \tag{2}$$

where r_{rated} indicates the rated intensity of solar radiation, and P_{PVr} indicates the rated output power of photovoltaic power generation.

(2) Wind power generation

Since the output power of wind power generation mainly varies with the wind speed at the location of the wind farm, and the wind speed is affected by the humidity of the environment, the weather, and the terrain where the wind farm is located, which is uncontrollable, wind power generation is also characterized by a certain degree of volatility and rapid change. However, in a longer time scale, the wind speed in most areas obeys the Weibull distribution, and its probability density function is expressed as equation (3):

$$f(v) = \frac{k}{c}\left(\frac{v}{c}\right)^{k-1} e^{-(v/c)^k} \tag{3}$$

where $f(v)$ is the probability density function of wind speed, v is the wind speed, and k and c are the shape and scale parameters of the Weibull distribution, respectively, which are expressed as Eqs. (4) and (5):

$$k = \left(\frac{s_W}{m_W}\right)^{1086} \tag{4}$$

$$c = \frac{2m_w}{\sqrt{p}} \tag{5}$$

where s_w and m_w are the standard deviation and mean of the wind speed, respectively.

The actual wind power output P_w varies with the wind speed at the location of the WTGs, which is expressed in equation (6):

$$P_W = \begin{cases} 0 & v \le V_{c1} \le V_{co} \\ P_{Wr}\dfrac{v - V_{c1}}{V_r - V_{c1}} & V_{c1} \le v \le V_r \\ P_{Wr} & V_r \le v \le V_{co} \end{cases} \tag{6}$$

where P_{wr} represents the rated power of the wind turbine and V_{cl}, V_{co}, V_r represents the cut-in, cut-out and rated wind speed of the wind turbine, respectively.

(3) Gas turbine

Gas turbine is a controllable power source, which is an effective auxiliary unit for renewable energy into the grid, and can smooth out the randomness and volatility of wind power and photovoltaic output. Has the flexibility of regulation, but in the gas generating unit operation stage, the gas turbine power generation can not exceed the maximum power generation of the gas turbine, expressed as equation (7):

$$0 \leq P_{g,t} \leq P_{g,\max} \tag{7}$$

where $P_{g,t}$ denotes the power generated by the gas turbine at the t moment, and $P_{g,\max}$ denotes the maximum power generated by the gas turbine.

II. B. 3) Source loads

If a large number of PV and wind units are connected to the VPP, the stability of the VPP will be seriously affected due to the stochastic and fluctuating nature of PV and wind power generation, which can be utilized in addition to gas turbines, and source loads can also be used. Source load is a kind of load with two-way energy interaction, which can be used as a power source to deliver active power to the VPP, and also as a load to dissipate renewable energy output, mainly including energy storage and electric vehicles (EVs).

This chapter mainly takes the battery as an example to analyze the characteristics of distributed energy storage. The charging state of the battery is constantly changing during the charging and discharging process, and the charging state at the moment of t is expressed as equations (8) and (9):

$$SOC_{t+1} = (1-d)SOC_t + \frac{P_{c,t}h_c}{E_s}\Delta t \tag{8}$$

$$SOC_{t+1} = (1-d)SOC_t - \frac{P_{d,t}h_d}{E_s}\Delta t \tag{9}$$

In the formula, SOC_t and SOC_{t+1} are the state of charge at t and $t+1$ moments, respectively, $P_{c,t}$ and $P_{d,t}$ are the charging and discharging power, h_c and h_d are the charging and discharging efficiencies, respectively, and d is the self-discharging rate of the battery. The state of charge and the charging/discharging power are subject to the following constraints:

$$SOC_{\min} \leq SOC_t \leq SOC_{\max} \tag{10}$$

$$0 \leq P_{c,t} \leq P_{c,\max} \tag{11}$$

$$0 \leq P_{d,t} \leq P_{d,\max} \tag{12}$$

where $SOC_{\max}$ and $SOC_{\min}$ denote the upper and lower limits of the charging state, and $P_{c,\max}$ and $P_{d,\max}$ denote the upper limits of charging and discharging, respectively.

III. Resource aggregation scheduling and optimization control strategy for virtual power plants

This chapter investigates the resource aggregation scheduling and optimization control strategy of virtual power plants (VPPs) with combined heat and power (CHP), and establishes an optimal scheduling method for VPPs based on the decoupling of “heat to power”. The VPP in this chapter covers all thermal power plants, wind farms and photovoltaic power plants in the region.

III. A. VPP mode of operation

The VPP uses a coordination and control center to collect various types of information from various subordinate energy units such as thermal power plants and wind power stations, and connects the information base with the information database of the large power grid to participate in the operation and scheduling of the large power grid. The heat storage electric boiler obtains abandoned wind and light power from the VPP through the interface unit and converts it into heat output to supply heat to the district heating network. The energy storage battery is connected to the VPP power system through the interface unit, in the form of charging and discharging, to mitigate the impact of fluctuating wind and photovoltaic new energy sources when they are connected to the grid. The thermal power plant is connected to the power system and district heating network in the VPP respectively, and the power is supplied to the VPP through the interface unit, and the heat output can be directly transported to the district heating network, and the heat storage device is used to store the excess heat, and the heat storage device utilizes the remaining heat to supply heat to the district heating network when the wind and light new energy output is in

excess, realizing the purpose of “Thermoelectrolysis Coupling”. The purpose of “thermal electrolysis coupling” is realized.

III. B. Optimized scheduling model

III. B. 1) Objective function

With the objective of optimal economy and lowest rate of wind and light abandonment in one dispatch cycle of VPP, its power generation cost includes coal consumption cost, environmental protection cost, cost of wind and light power generation kWh, investment and construction cost and operation and maintenance cost of heat storage device, thermal storage electric boiler and storage battery, in which the penalty of wind and light abandonment is set in order to satisfy the requirement of high utilization of wind and light, and the income is the revenue from the sale of electricity of VPP and heat supply revenue, and the objective function is:

$$\max F = I_{sale}^{k} - C_{coal}^{k} - C_{wind}^{k} - C_{pv}^{k} - C_{chu} - C_{xu} - C_{pb} - C_{pc}^{k} - C_{hb}^{k} - C_{qi}^{k} \tag{13}$$

where, F is the economic benefit of the VPP in a dispatch cycle, and the meanings of the rest of the items in equation (13) are listed below:

(1) I_{sale}^{k} denotes the revenue from the sale of electricity and heat from the virtual power plant to the grid and the heat supply network in time period k, expressed as follows:

$$I_{sale}^{k} = a(k)\left(p_{wind}^{k} + p_{pv}^{k} + P_{pb}^{k} + \sum_{i \in q} p_{CHP}^{ik}\right) + b\left(\sum_{i \in q} H_{CHP}^{ik} + H_{chu}^{k} + H_{xu}^{k}\right) \tag{14}$$

where, i denotes the number of the cogeneration unit, p_{wind}^{k}, p_{pv}^{k} is the electricity output of the wind farm and photovoltaic plant in time period k, $p_{CHP}^{ik}, H_{CHP}^{ik}$ is the electricity output and heat output of the i th unit in time period k, P_{m}^{k} denotes the electricity output of the storage battery, H_{chu}^{k}, H_{xu}^{k} is the heat output of the heat storage device and heat storage electric boiler, $a(k)$ denotes the price of the electricity sold, which is a fixed tariff, and b denotes the price of the heat sold by the VPP.

(2) C_{coal}^{k} represents the cost of electricity and heat production of a thermal power plant, which includes the cost of coal consumption and the cost of operation and maintenance, expressed as follows:

$$C_{coal}^{k} = x_1 \sum_{i \in q} p_{CHP}^{k} + x_2 \sum_{i \in q} H_{CHP}^{k} \tag{15}$$

where, x_1, x_2 is the cost coefficient of electricity and heat production of the CHP unit, respectively, which includes the cost of coal consumption and the cost of operation and maintenance.

(3) C_{wind}^{k} denotes the total electricity generation unit cost of the wind farm in time period k:

$$C_{wind}^{k} = \frac{c_w p_{wind}^{k}}{4} \tag{16}$$

where, c_w represents the unit generation cost of the wind farm in yuan/(MW · h).

(4) C_{pv}^{k} is the generation cost of the PV power plant in the kth time period:

$$C_{pv}^{k} = \frac{c_{pv} p_{pv}^{k}}{4} \tag{17}$$

where, c_{pw} is the unit power generation cost of the PV plant in yuan/(MW · h).

(5) C_{chu} is the investment construction and operation and maintenance cost of the heat storage device, converted to day:

$$C_{chu} = \frac{Q_{chure} r_{chure} (1 + d_{chure})}{365 \times n} \tag{18}$$

where, Q_{chure} indicates the heat storage capacity of the heat storage device, r_{chure}, d_{chure} indicates the unit capacity cost of the heat storage tank as well as the operation and maintenance cost, respectively, n indicates the service life, and this chapter takes n as 40 years.

(6) C_{xu} represents the investment construction and operation and maintenance costs of the heat storage electric boiler, converted to days:

$$C_{xu} = \frac{Q_{xu} r_{xu} (1 + d_{xu})}{365 \times n} \tag{19}$$

where, Q_{xu} indicates the capacity of the thermal storage electric boiler, r_{xu}, d_{xu} indicates the unit capacity cost of the thermal storage electric boiler and the operation and maintenance cost, respectively, n indicates the service life, and this chapter takes n as 20 years.

(7) C_{R_h} represents the investment construction and operation and maintenance costs of the storage battery, converted to days:

$$C_{p_b} = \frac{Q_{p_b} r_{p_b} (1 + d_{p_b})}{365 \times n} \tag{20}$$

were, Q_{p_b} denotes the capacity of the storage battery, r_{p_b}, d_{p_b} denotes the cost per unit capacity of the storage battery and the operation and maintenance cost, n denotes the service life, and in this paper, we take n as 15 years.

(8) C_{pe}^{k} is the penalty cost for the deviation of the actual output of the virtual power plant from the planned output in time period k :

$$C_{pe}^{k} = g \left| P_{VPP}^{k} - \sum_{i \in q} P_{CHP}^{ik} - P_{wind}^{k} - P_{pv}^{k} - P_{ps}^{k} \right| \tag{21}$$

where, g is the VPP output deviation penalty coefficient, and P_{vpp}^{k} is the planned VPP output for the k time period.

(9) C_{hb}^{k} is the environmental protection cost of the k -time period VPP, which is calculated based on the amount of pollutants emitted by the CHP unit during operation and the environmental protection cost of the pollutants corresponding to each pollutant:

$$C_{hb}^{k} = \sum_{j=1}^{m} \left[v_{ej} d_{ej} \sum_{i \in q} \left(\frac{P_{CHP}^{ik} + H_{CHP}^{ik}}{4} \right) + v_j \right] \tag{22}$$

where, m denotes the number of pollutants, v_{ej} denotes the unit environmental treatment cost of the j rd pollutant, d_{ej} denotes the emission of the pollutant, and v_j denotes the penalty cost of generating the j th pollutant.

(10) C_{qi}^{k} represents the penalty for wind and light abandonment:

$$C_{qi}^{k} = g(P_{wind-pv}^{k,plan} - P_{wind-pv}^{k,real}) \tag{23}$$

where, g represents the unit penalty price for virtual power plant wind and light abandonment, $P_{wind-pv}^{k,plam}$ represents the planned output of wind and light, and $P_{wind-p}^{k,real}$ represents the actual output of wind and light.

III. B. 2) Constraints

(1) Electrical power balance constraints:

$$P_{need}^{k} = \sum_{i \in q} P_{CHP}^{ik} + P_{wink}^{k} + P_{pv}^{k} + P_{b}^{k} \tag{24}$$

(2) Thermal power balance constraints:

$$H_{need}^{k} = \sum_{i \in q} H_{CHP}^{ik} + H_{chu}^{k} + H_{eh}^{k} \tag{25}$$

(3) CHP unit electrical and thermal output and climb constraints:

$$p_{CHP}^{¢} \le p_{CHP}^{¢} \le p_{CHP}^{¢} \begin{cases} p_{CHP}^{¢\min} \le p_{CHP}^{¢} \le p_{CHP}^{¢\max} \\ H_{CHP}^{¢\min} \le H_{CHP}^{¢} \le H_{CHP}^{¢\max} \\ -R_{CHP}^{¢\min} \le p_{CHP}^{¢} - p_{CHP}^{¢} \le R_{CHP}^{¢\max} \end{cases} \tag{26}$$

where, $R_{CWP}^{¢}$ and $R_{CWP}^{¢}$ denote the absolute value of the so-small and maximum creep rate of the red generation power of the i rd CHP machine, respectively.

(4) Thermoelectric unit operating characteristic constraints:

There exists a specific thermoelectric operation interval for the pumped CHP unit, which can be used to characterize its thermoelectric coupling characteristics:

$$\begin{cases} p_{CHP}^{med} + C_{l1}^{'} H_{CHP}^{ik} \le p_{CHP}^{ik} \le p_{CHP}^{¢\max} + C_{l2}^{'} H_{CHP}^{ik}, 0 \le H_{CHP}^{ik} \le H_{CHP}^{¢\max} \\ p_{CHP}^{¢\min} + C_{m}^{'} (H_{CHP}^{ik} - H_{CHP}^{¢med}) \le p_{CHP}^{ik} \le p_{CHP}^{¢\max} + C_{l2}^{'} H_{CHP}^{ik}, H_{CHP}^{¢med} \le H_{CHP}^{ik} \le H_{CHP}^{¢\max} \end{cases} \tag{27}$$

where, $C_{l1}^{¢}, C_{l2}^{¢}$ represents the change in the minimum and maximum electrical output of the unit for each unit of heat generated by the i nd extraction CHP unit, respectively, and $C_{m}^{¢}$ represents the change in the minimum electrical output of the unit for each unit of heat generated by the i th extraction CHP unit in backpressure operation.

III. B. 3) Additional energy storage unit model and constraints

1) Lithium-ion storage battery model:

$$p_b(k) = \begin{cases} \dfrac{p_{b0}(k)}{h_{ES,d}} & p_{bis}(k) \ge 0 \\ p_{bis}(k) h_{ES,c} & p_{bis}(k) < 0 \end{cases} \tag{28}$$

where, $p_b(k)$ is the power required to smooth the fluctuation of new energy output, the value is positive for the storage battery discharge, the value is negative for the storage battery charging, $h_{ES,e}, h_{ES,d}$ represents the battery charging and discharging efficiency, respectively, in this chapter take $h_{ES,c} = h_{ES,d} = 90\%$.

Constraints:

(1) Capacity constraints:

$$\begin{cases} E(k) = E(k-1) - p_b(k) \\ 0 < E(k) < Q_{ESS} \end{cases} \tag{29}$$

where, E is the power within the energy storage system and Q_{ESS} is the capacity of the energy storage device.

(2) Power constraint:

$$p_{b\_c,\max} \le p_b(k) \le p_{b\_f,\max} \tag{30}$$

where, $p_{b\_c,\max}, p_{b\_f,\max}$ is the maximum charging and discharging power of the energy storage battery respectively.

(3) Energy storage battery operation constraints:

$$\Delta E = \sum_{k=1}^{96} \frac{p_b(k) T_s}{60} = 0 \tag{31}$$

where, T_s is the sampling period in min, $\mathrm{D}E$ indicates the difference between the power in the battery and the power in the battery before the start of the cycle after the energy storage battery completes the complete operation of a cycle in kw·h, and $\mathrm{D}E = 0$ is to ensure that the energy storage battery can operate continuously in a safe and stable manner.

2) Heat storage electric boiler model:

$$P_{eh,k}C_{eh} = H_{in,k} + H_{d,k} \tag{32}$$

In the formula: $P_{eh,k}$ indicates the electric heating power of the electric heating system, $H_{d,k}, H_{in,k}$ indicates the direct heating power and heat storage power of the electric boiler, respectively, and C_{eh} indicates the electric heat conversion coefficient, which is taken as $C_{eh} = 1$.

Electric power constraints for electric boilers:

$$0 \leq P_{ch,k} \leq P_{ch}^{\max} \tag{33}$$

where, $P_{ch}^{\max}$ indicates the maximum power of electric heating of electric boilers.

(3) Heat storage device model:

(1) Capacity constraint:

$$0 \leq S_k \leq S_{\max} \tag{34}$$

where, $S_{\max}$ indicates the maximum heat storage capacity of the thermal storage tank.

(2) Storage and discharge heat power constraints:

$$\begin{cases} 0 \leq H_{in_{r,k}} \leq H_{in}^{\max} \\ 0 \leq H_{out,k} \leq H_{out}^{\max} \end{cases} \tag{35}$$

(3) State constraints:

$$\begin{cases} \mathrm{D}t(H_{in,k} - H_{outk} - k_{1oss}S_k) = S_{k+1} - S_k \\ S_N = S_0 \end{cases} \tag{36}$$

where, S_N represents the heat in the heat storage tank after the Nth time period.

III. B. 4) Methods for solving the model

The above optimization problem is a mixed integer nonlinear optimization problem containing quadratic terms, and the constraints of electricity and heat affect each other, the source, load and storage resources are related to each other, and the constraints of heat load are dynamic intervals, and the improved Particle Swarm Algorithm is considered to be used to solve the problem. Particle swarm optimization algorithm (PSO) is a stochastic search algorithm that simulates the phenomenon of bird foraging in nature, and is widely used in various engineering optimization problems due to its strong optimization capability and simplicity. The flock of birds is analogous to a set of effective solutions in the search space, the foraging space is analogous to the feasible domain of the optimization problem, the flight speed and location of the flock are analogous to the velocity and position vectors of the solution, and the individual cognition and group collaboration in the flock are analogous to the efficiency of updating the velocity and position of the particles, and the end of the foraging process represents the finding of a globally optimal solution of the optimization problem.

Let the number of particles in the flock be M, the dimension of the particle's motion space be D, the position of the i nd particle at moment t, and the velocity be as follows:

$$X_i = (x_{i1}, x_{i2}, \cdots, x_{iD}), i = 1, 2, \cdots, M \tag{37}$$

$$V_i = (v_{i1}, v_{i2}, \cdots, v_{iD}), i = 1, 2, \cdots, M \tag{38}$$

At each moment, the location of the optimal solution currently found by the entire population and the location of the optimal solution currently found by each particle are saved in the particle swarm based on their respective fitness function values. Then iterations are performed to update the velocity and position of each particle at the next moment. Then:

$$\begin{aligned} v_i &= wv_i + c_1 r_1 (p_i - x_i) + c_2 r_2 (p_g - x_i) \\ x_i &= x_i + v_i \end{aligned} \tag{39}$$

$$w = w_{\max} - (w_{\max} - w_{\min}) \frac{iter}{ger} \tag{40}$$

In the above equation, w is the inertia weight, which is expressed in the standard PSO algorithm as shown in (40), c_1, c_2 is the learning factor, p_i is the optimal solution of the particle, p_x is the optimal solution of the population, r_1, r_2 is the random number in the range of [0, 1], $iter, ger$ is the current number of iterations and the set maximum number of iterations, respectively, and $w_{\max}, w_{\min}$ is the range of the set change of inertia weight, which can be generally taken as [0.4, 0.9].

Improvement of the standard PSO algorithm can accelerate the search and convergence efficiency of the particles and increase its ability to find the global optimal solution. Among them, the PSO algorithm with improved inertia weights has been widely used in engineering practice because inertia weights are the most critical parameter to determine the efficiency of particle swarm search. In this chapter, the PSO algorithm with adaptive weights is used to solve the problem. The improved inertia weights are calculated as shown in Eq. (41) below, where f represents the fitness function value (i.e., the optimization objective) of the particle, and $f_{\min}$ and f_{avg} are the optimal and average values of the swarm, respectively:

$$w = \begin{cases} w_{\min} - \dfrac{(w_{\max} - w_{\min})(f - f_{\min})}{(f_{avg} - f_{\min})} & f \le f_{avg} \\ w_{\max} & f > f_{avg} \end{cases} \tag{41}$$

IV. Analysis of examples

IV. A. Data acquisition

In order to validate the effectiveness of the optimal scheduling model for virtual power plant resources, the improved IEEE 30 node test system is selected as an example in this section. The IEEE 30 bus system is used as an example by replacing the node data and load characteristics. Specifically, in the original system, bus 15 is replaced with wind power generation, bus 23 with photovoltaic (PV) generation, buses 1 & 2 with conventional power plants, and buses 22 & 27 with cogeneration units. Temporal and spatial data such as wind speed data, PV irradiance data, electrical load, thermal load, and tariffs are selected for the system during a typical day in winter.

IV. B. Algorithm Optimization Performance

The results of the improved PSO and GA algorithms for optimal scheduling of virtual power plant resources are analyzed separately, using cost control as a reference. In order to observe the influence of the variables of control parameters in the two algorithms on the convergence of the optimization results, two scenarios with different parameters are set up:

(1) The number of particles, individual acceleration factor and social acceleration factor of the improved PSO algorithm are 20, 2, 2. The number of individuals, crossover probability and variance probability of the GA algorithm are 60, 0.80, 0.025.

(2) The number of particles, individual acceleration factor and social acceleration factor of the improved PSO algorithm are 30, 3, 3. The number of individuals, crossover probability and variance probability of the GA algorithm are 85, 0.83, 0.04.

The convergence of the two algorithms in the two scenarios is analyzed, and the convergence of the two algorithms in scenario one and scenario two is shown in Figures 2 and 3. The improved PSO algorithm converges to 26830.64 yuan and 26830.54 yuan in case I and case II respectively, while the GA algorithm converges to 26859.84 yuan and 26855.85 yuan, and the improved PSO algorithm obtains the optimal solution faster in the calculation process.

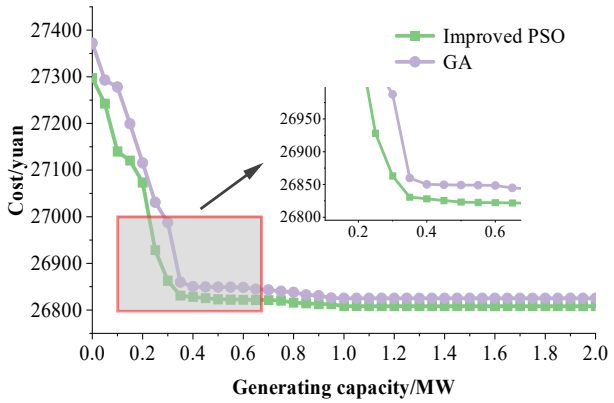

Figure 2: The convergence of two algorithms in the case 1

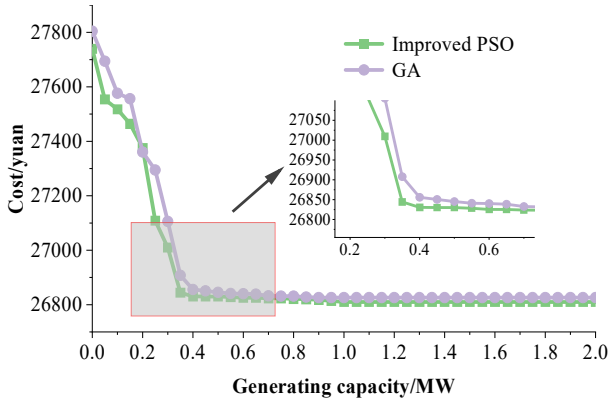

Figure 3: The convergence of two algorithms in the case 2

In addition, the optimal solutions of the two algorithms are analyzed in two scenarios. In scenario 1, the VPP generation cost does not include the distribution network reactive power compensation cost. The two algorithms are used to solve the objective function, and the optimal cost of generation investment in this case can be obtained. Comparison of the results of the two algorithms in Case 1 is shown in Figure 4, compared with the GA algorithm, the optimal cost of a single unit obtained by the improved PSO algorithm is lower, and the final total investment cost of the improved PSO algorithm and the GA algorithm are 26,829.21 yuan and 26,847.16 yuan, respectively.

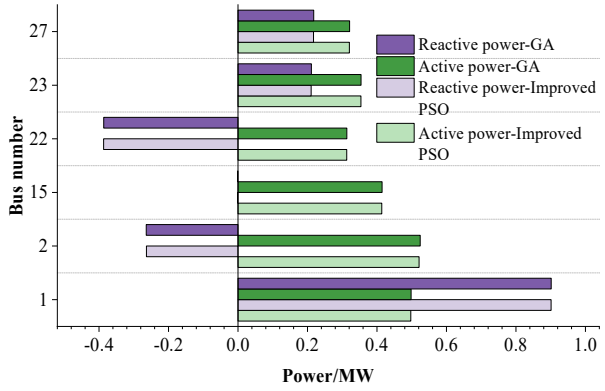

Figure 4: The calculation result of the two algorithms in the case 1

The final optimization result of the objective function in case two, considering its influence on the system parameters and constraints, is shown in Fig. 5. The optimal cost of the two cases calculated by the improved PSO algorithm is 26827.82 yuan, while the optimal cost of the GA algorithm is 26853.47 yuan, so the improved PSO algorithm calculates the result obviously better.

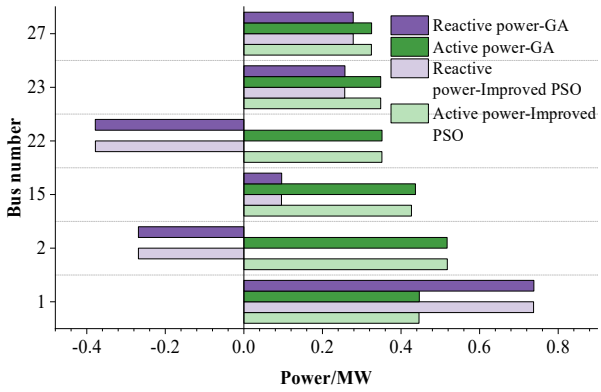

Figure 5: The calculation result of the two algorithms in the case 2

IV. C. Analysis of storage configuration results

The relationship between the annual profit of the virtual power plant as a function of the capacity of the electrical and thermal energy storage is shown in Figure 6. The annual profit of the virtual power plant varies with the configured capacity of the electrical and thermal energy storage. For thermal energy storage, when the capacity of thermal energy storage is in the range of 25 MWh to 45 MWh, the annual profit of the virtual power plant is higher than that of the other configuration cases. However, the increase in the annual profit of the virtual power plant is not significant when the capacity of thermal energy storage is increased from 15 MWh to 55 MWh. For electric energy storage, on the other hand, as the configured capacity varies in the range of 4MWh to 9MWh, the annual profit of the virtual power plant increases with the increase in capacity until the electric energy storage reaches the upper limit of the configured capacity. In addition, each 1MWh increase in electric storage capacity brings a larger value-added annual profit of the virtual power plant. Therefore, the scientific allocation of energy storage facilities in the virtual power plant planning can help the virtual power plant to gain greater profit.

From the calculation of the example, the optimal configuration capacity of electric energy storage is 9 MWh, and the optimal configuration capacity of thermal energy storage is 35 MWh. in this case, the virtual power plant obtains the maximum annual profit, which is increased by 600,561,000 yuan compared with the case of not installing energy storage facilities.

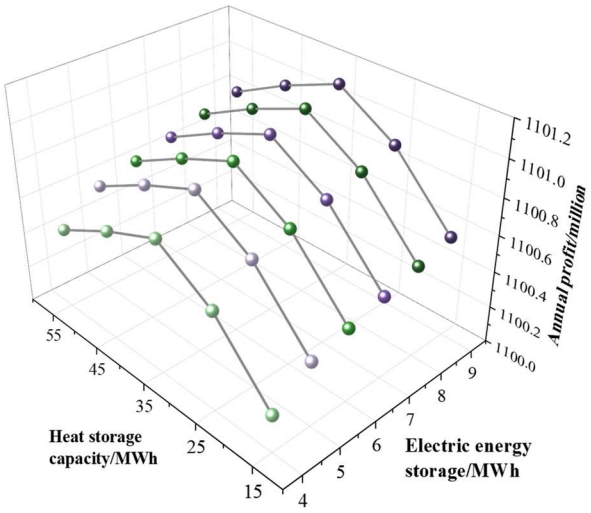

Figure 6: Annual profit varies with the electric energy storage and heat storage capacity

IV. D. Analysis of optimized scheduling results

Taking a characteristic day in winter as an example, the results of the optimal allocation of the virtual power plant's electric and thermal energy storage are substituted in the model to analyze the optimal dispatching scheme for each moment within the virtual power plant. Figure 7 shows the electric output of the virtual power plant, and the total electric output power of the unit remains basically constant at around 250 MW. This shows that under the conditions of electric and thermal energy storage and integrated demand response, the “heat and power coupling”

phenomenon of the CHP unit is alleviated, thus increasing the unit's electric output variation range. For power market clearing, between 0:00 and 7:00 and between 22:00 and 24:00 at night, the total power output of the distributed resources within the virtual power plant is greater than the load value, so the virtual power plant sells the excess power to the power market for revenue. Between 8:00 and 21:00, the electric load value of the virtual power plant is larger, and the total electric output of the internal distributed resources is smaller than the electric load value, so the virtual power plant needs to purchase power from the power market to achieve power balance. It can be seen that the power output is balanced at all moments during the 24-hour dispatch cycle.

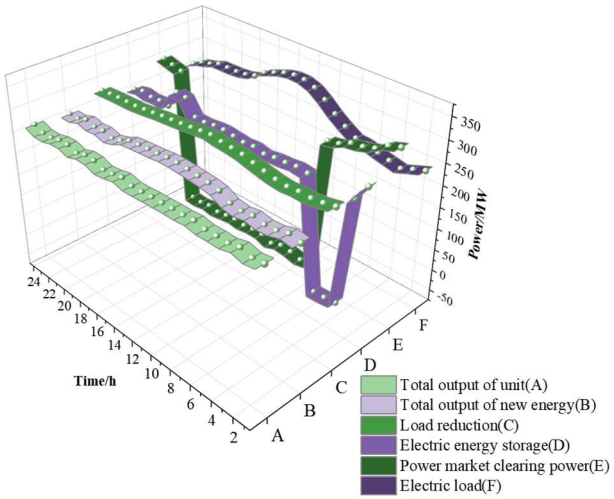

Figure 7: Electrical power output of virtual power plants

Figure 8 shows the heat output of the virtual power plant. The total output thermal power of the unit is similar to the trend of the thermal load, and the demand for the thermal output of the CHP unit is always higher in winter, and its thermal output value of the unit exceeds the value of the thermal load between 4:00 and 5:00 and between 21:00 and 24:00. When the thermal output of the unit is greater than the thermal load value, the excess thermal output at this time is fed into the thermal energy storage equipment for storage. At the rest of the time, when the thermal output of the unit is less than the thermal load value, the thermal energy storage releases heat to maintain the thermal balance in the virtual power plant. Therefore, after the configuration of thermal energy storage equipment in the virtual power plant, the thermal output of the virtual power plant can be balanced, so that the “thermo-electric coupling” phenomenon of the cogeneration unit can be alleviated and the flexibility of the virtual power plant can be increased.

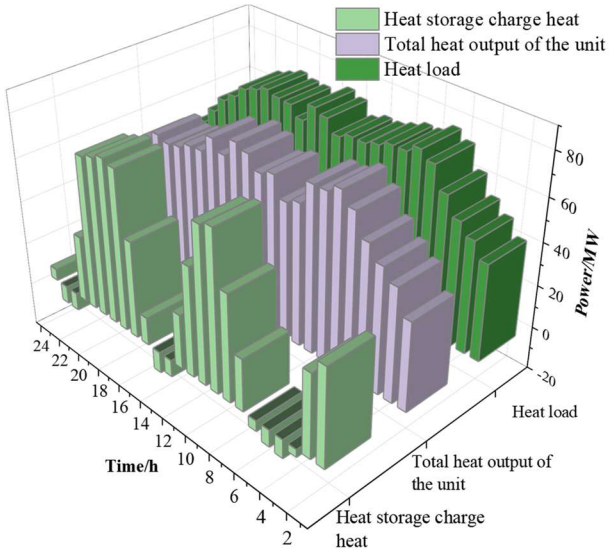

Figure 8: The heat output of the virtual power plant

The electrical and thermal energy storage outputs are shown in Figure 9. The electric energy storage releases power at 1:00, stores power from 3:00 to 6:00, and releases power from 18:00 to 21:00. This is because during this period, the sum of the total electrical output of the units and new energy sources in the virtual power plant is less than the electrical load value, which needs to be balanced by either the electrical storage output or the electrical load demand response. Thermal energy storage stores thermal energy from 3:00 to 6:00, 13:00 to 14:00, and 22:00 to 23:00, and releases thermal energy from 9:00 to 10:00 and 17:00 to 19:00, because the cost of charging and discharging with thermal energy storage is lower, and so thermal energy storage is preferred to maintain the thermal balance of the virtual power plant. In summary, electrical and thermal energy storage can effectively mitigate the multi-energy coupling characteristics of virtual power plants, thus improving the flexibility and profitability of virtual power plants.

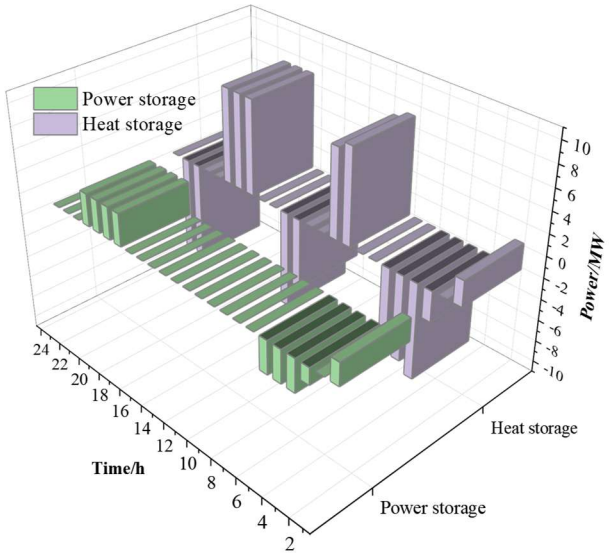

Figure 9: The output of power storage and heat storage

V. Conclusion

With the continuous development and progress of the energy industry, virtual power plants will be more widely used. This paper models the virtual power plant resources and their characteristics, and proposes a virtual power plant resource optimization scheduling model based on “heat to set electricity” for the virtual power plant resource scheduling of hotspot union, which is solved by the improved particle swarm algorithm. It is found that the optimized model using the improved particle swarm algorithm is more economical than the GA algorithm, and the optimal cost is about 26830 yuan. The optimal configuration of electrical and thermal energy storage is 9MWh and 35MWh respectively, and the annual profit of the virtual power plant under this configuration can be improved by 605,610,000 yuan. The total power output of the unit is stabilized at about 250MWh after optimal scheduling, and the phenomenon of “thermo-electric coupling” is alleviated at the same time. The analysis shows that the proposed optimal scheduling model is able to combine the two means of electric and thermal energy storage configuration and integrated demand response to realize the decoupling of heat and power relationship of the virtual power plant, at the same time, satisfy the internal resource characteristics of the virtual power plant, improve the electric and thermal regulation capability of the virtual power plant, increase the profit of the virtual power plant, and promote the safe and reliable operation of the power system.

The virtual power plant has the advantages of distributed flexible and adjustable resource aggregation in a wider area and more decentralized configuration, which is more adaptable to the characteristics of the future distributed resource blowout disorderly access to the medium and low voltage distribution network. In the future, further research can be conducted on the multilevel coordination and optimization of virtual power plant resources to achieve efficient and synergistic resource allocation.

Funding

This work was supported by ChangChun Finance College “Research on Optimization Strategy of Campus Data Center Based on Cloud Computing” Project No 2024JZ016.

References

[1] Zhou, Y., Wang, C., Wu, J., Wang, J., Cheng, M., & Li, G. (2017). Optimal scheduling of aggregated thermostatically controlled loads with renewable generation in the intraday electricity market. Applied energy, 188, 456-465.

[2] Appino, R. R., Hagenmeyer, V., & Faulwasser, T. (2021). Towards optimality preserving aggregation for scheduling distributed energy resources. IEEE Transactions on Control of Network Systems, 8(3), 1477-1488.

[3] Fonseca, T., Ferreira, L. L., Landeck, J., Klein, L., Sousa, P., & Ahmed, F. (2022). Flexible loads scheduling algorithms for renewable energy communities. Energies, 15(23), 8875.

[4] Gržanić, M., & Capuder, T. (2021). Coordinated scheduling of renewable energy balancing group. International Journal of Electrical Power & Energy Systems, 125, 106555.

[5] Mi, Z., Jia, Y., Wang, J., & Zheng, X. (2018). Optimal scheduling strategies of distributed energy storage aggregator in energy and reserve markets considering wind power uncertainties. Energies, 11(5), 1242.

[6] Gomes, I. L. R., Melicio, R., Mendes, V. M. F., & Pousinho, H. M. I. (2019). Decision making for sustainable aggregation of clean energy in day-ahead market: Uncertainty and risk. Renewable Energy, 133, 692-702.

[7] Li, S., Xu, Q., Yang, Y., Xia, Y., & Hua, K. (2024). Study on distributed renewable energy generation aggregation application based on energy storage. International Journal of Electrical Power & Energy Systems, 158, 109935.

[8] Singh, S., Singh, M., & Kaushik, S. C. (2016). Optimal power scheduling of renewable energy systems in microgrids using distributed energy storage system. IET Renewable Power Generation, 10(9), 1328-1339.

[9] Ullah, Z., Mokryani, G., Campean, F., & Hu, Y. F. (2019). Comprehensive review of VPPs planning, operation and scheduling considering the uncertainties related to renewable energy sources. IET Energy Systems Integration, 1(3), 147-157.

[10] Yi, Z., Xu, Y., Gu, W., & Wu, W. (2019). A multi-time-scale economic scheduling strategy for virtual power plant based on deferrable loads aggregation and disaggregation. IEEE Transactions on Sustainable Energy, 11(3), 1332-1346.

[11] Ayón, X., Gruber, J. K., Hayes, B. P., Usaola, J., & Prodanović, M. (2017). An optimal day-ahead load scheduling approach based on the flexibility of aggregate demands. Applied Energy, 198, 1-11.

[12] Zhang, T., & Hu, Z. (2021). Optimal scheduling strategy of virtual power plant with power-to-gas in dual energy markets. IEEE Transactions on Industry Applications, 58(2), 2921-2929.

[13] Wu, C., Fang, L., Yang, T., Zhang, F., & Qiu, Y. (2024, July). Virtual Power Plant Response Strategy Considering Dynamic Aggregation of Different Flexible Resources. In Journal of Physics: Conference Series (Vol. 2774, No. 1, p. 012044). IOP Publishing.

[14] Baringo, A., Baringo, L., & Arroyo, J. M. (2018). Day-ahead self-scheduling of a virtual power plant in energy and reserve electricity markets under uncertainty. IEEE Transactions on Power Systems, 34(3), 1881-1894.

[15] Li, Q., Zhou, Y., Wei, F., Li, S., Wang, Z., Li, J., ... & Yu, D. (2024). Multi-time scale scheduling for virtual power plants: Integrating the flexibility of power generation and multi-user loads while considering the capacity degradation of energy storage systems. Applied Energy, 362, 122980.

[16] Li, J., Mo, H., Sun, Q., Wei, W., & Yin, K. (2024). Distributed optimal scheduling for virtual power plant with high penetration of renewable energy. International Journal of Electrical Power & Energy Systems, 160, 110103.

[17] Pan, P., Zhao, M., Gao, Y., Wang, X., Zhao, Y., & Ma, H. (2024, May). Flexible Resource Virtual Power Plant Aggregation Scheduling Method Considering Uncertainty and Demand Response. In 2024 Second International Conference on Cyber-Energy Systems and Intelligent Energy (ICCSIE) (pp. 1-6). IEEE.

[18] Qiu, J., Meng, K., Zheng, Y., & Dong, Z. Y. (2017). Optimal scheduling of distributed energy resources as a virtual power plant in a transactive energy framework. IET Generation, Transmission & Distribution, 11(13), 3417-3427.

[19] Dou, X., Wang, J., Wang, Z., Ding, T., & Wang, S. (2021). A decentralized multi-energy resources aggregation strategy based on bi-level interactive transactions of virtual energy plant. International Journal of Electrical Power & Energy Systems, 124, 106356.

[20] Chen, Q., Lyu, R., Guo, H., & Su, X. (2024). Real-time operation strategy of virtual power plants with optimal power disaggregation among heterogeneous resources. Applied Energy, 361, 122876.

[21] Liu, X., Lin, X., Qiu, H., Li, Y., & Huang, T. (2024). Optimal aggregation and disaggregation for coordinated operation of virtual power plant with distribution network operator. Applied Energy, 376, 124142.

[22] Cheng, L., Zhou, X., Yun, Q., Tian, L., Wang, X., & Liu, Z. (2019, November). A review on virtual power plants interactive resource characteristics and scheduling optimization. In 2019 IEEE 3rd Conference on Energy Internet and Energy System Integration (EI2) (pp. 514-519). IEEE.

[23] Subramanya, R., Yli-Ojanperä, M., Sierla, S., Hölttä, T., Valtakari, J., & Vyatkin, V. (2021). A virtual power plant solution for aggregating photovoltaic systems and other distributed energy resources for northern european primary frequency reserves. Energies, 14(5), 1242.

[24] Xu, B., Luan, W., Yang, J., Zhao, B., Long, C., Ai, Q., & Xiang, J. (2024). Integrated three-stage decentralized scheduling for virtual power plants: a model-assisted multi-agent reinforcement learning method. Applied Energy, 376, 123985.

[25] Jia, Z., Sun, Q., Wang, L., Chen, S., Gong, T., Ge, X., ... & Chen, Q. (2024, July). Low-Carbon and Economic Scheduling Strategy for Virtual Power Plant Based on Complementary Characteristics and Aggregation Model of DER. In 2024 IEEE/IAS Industrial and Commercial Power System Asia (I&CPS Asia) (pp. 502-507). IEEE.

[26] Bai, X., Fan, Y., Hao, R., & Yu, J. (2024). Data-driven virtual power plant aggregation method. Electrical Engineering, 1-10.

[27] Chadokar, L., Kirar, M. K., Yadav, G. K., Salaria, U. A., & Sajjad, M. (2025). Aggregation and Bidding Strategy of Virtual Power Plant. Journal of Electrical Engineering & Technology, 20(1), 199-216.